Supporting Information

Recycling Spent Dry Cells into rGO/MnO_2 Nanocomposite for Advanced Supercapacitor Electrode

Othai Saha[1,3], Md Humayun Kabir[2]*, Md. Mazharul Islam[3], Md. Sanwar Hossain[1], Muhammad Shahriar Bashar[4], Md Yeasin Pabel[1], Sabina Yasmin[1]*

[1]Institute of National Analytical Research and Service (INARS), Bangladesh Council of Scientific and Industrial Research (BCSIR), Dhanmondi, Dhaka-1205, Bangladesh

[2]Institute of Food Science and Technology (IFST), Bangladesh Council of Scientific and Industrial Research (BCSIR), Dhanmondi, Dhaka-1205, Bangladesh

[3]Department of Chemistry, University of Dhaka, Dhaka-1000, Bangladesh

[4]Institute of Energy Research & Development (IERD), Bangladesh Council of Scientific and Industrial Research (BCSIR), Dhanmondi, Dhaka-1205, Bangladesh

*Corresponding author e-mail: sabinayasmin@bcsir.gov.bd

*Corresponding author e-mail: humayunkabir@bcsir.gov.bd

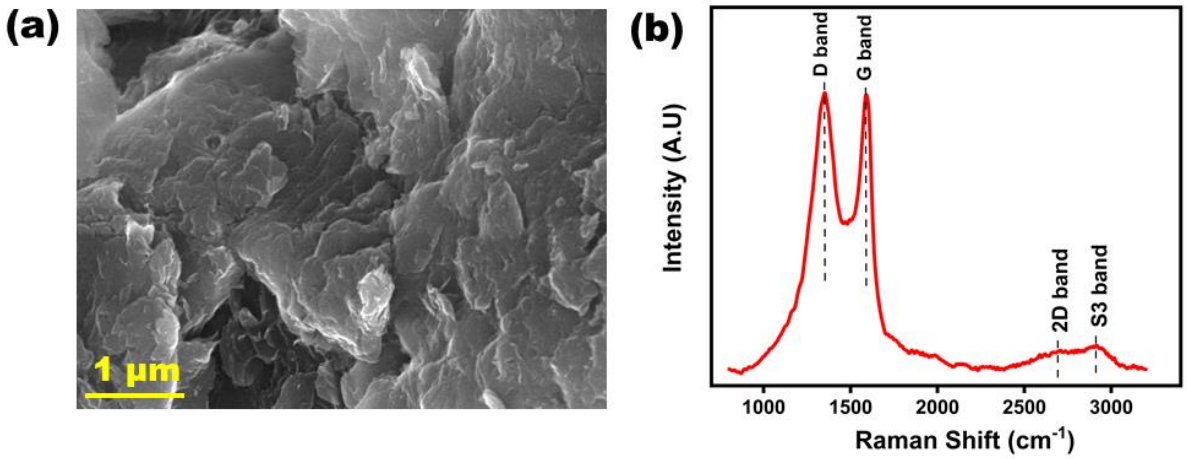

Fig. S1 SEM image of (a) GO and (b) Raman spectrum of GO

SEM of GO

The SEM image of graphene oxide (GO) in Fig. S1(a) exhibits its characteristic wrinkled and layered morphology. The sheets are stacked with irregular, rough edges, forming thin, flake-like structures. The folded surface is clearly visible, reflecting the effects of oxidation and the presence of oxygen-containing functional groups, consistent with findings reported in previous studies[1,2].

Raman Spectrum of GO

Figure S1(b) presents the Raman spectrum of graphene oxide (GO), highlighting the characteristic D, G, 2D, and S3 bands. The D band, observed at 1352 cm^{-1} for GO, arises from a disorder-induced breathing mode of k-point phonons with A_1g symmetry, reflecting defects such as vacancies, grain boundaries, or amorphous carbon [3]. The G band, located near 1590 cm^{-1}, corresponds to the E_2g phonon mode, representing the vibration of sp^2-hybridized carbon atoms [4]. The intensity ratio of these bands (I_D/I_G = 1.01) indicates a significant degree of structural disorder and a reduction in sp^2 domain size, consistent with lattice disruption caused by oxygen-containing functional groups [5–7]. The 2D band, observed around 2710 cm^{-1} in GO, provides information on layer number and stacking. In monolayer graphene, the 2D band appears as a sharp peak, whereas in multilayer graphene or GO, it becomes broadened and shifted due to defects and oxygen-induced disruption of interlayer interactions [2,3].

Additionally, the S3 band (2910 cm^{-1}), arising from D + G combination modes, provides further information on defect density and oxygen content. Collectively, these Raman features offer a comprehensive understanding of the structural disorder, layer number, and stacking characteristics of graphene-based materials [3,8].

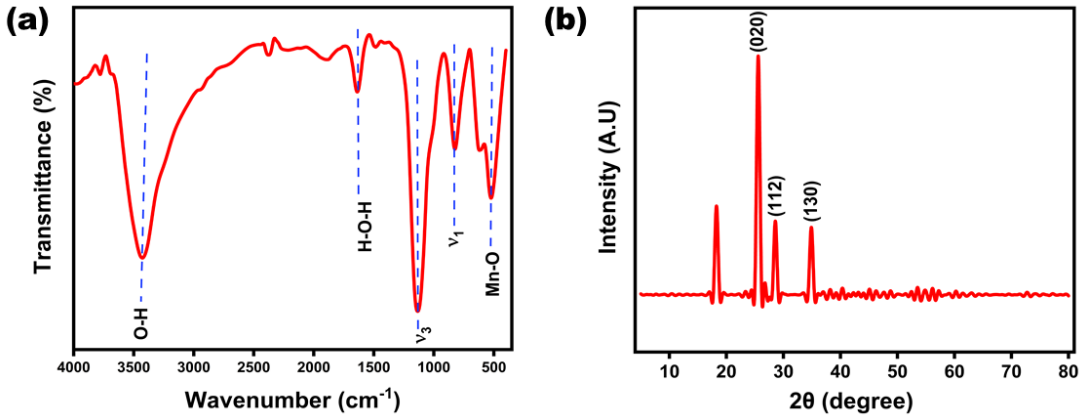

Fig. S2 (a) FT-IR and (b) XRD of $MnSO_4$

FT-IR Spectrum of $MnSO_4$

The FT-IR spectrum of pure $MnSO_4$ (Fig.S2(a)) displayed characteristic vibrational bands corresponding to sulfate groups, coordinated water molecules, and Mn-O bonding, confirming its structural identity. A prominent peak at 890 cm^{-1} was attributed to the ν_1 symmetric stretching vibration of the tetrahedral SO_4^{2-} anion, while a band at 1130 cm^{-1} corresponded to the ν_3 asymmetric stretching vibration, which is typically more complex and less intense than the symmetric mode. In the higher wavenumber region, a broad band centered around 3430 cm^{-1} was assigned to O-H stretching vibrations of coordinated water molecules, with its broadness indicative of hydrogen bonding that stabilizes the crystalline framework [9,10]. Additionally, a weaker band near 1630 cm^{-1} was associated with H-O-H bending vibrations, further confirming the presence of hydration water. In the low-frequency region, a doublet at 619 and 520 cm^{-1} corresponded to Mn-O vibrational modes, evidencing a strong metal-oxygen coordination environment. Collectively,

these spectral features including sulfate vibrations, O-H stretching and bending, and Mn-O lattice vibrations confirm the hydrated crystalline structure of $MnSO_4$ [9,10].

XRD of $MnSO_4$

The crystalline properties of pure $MnSO_4$ were examined using XRD analysis (Fig. S2(b)). The diffraction pattern displayed sharp and intense peaks at 25.38°, 28.37°, and 34.81°, which correspond to the (020), (112), and (130) crystal planes, respectively, and are in good agreement with the standard manganese sulfate diffraction pattern [11]. The high intensity and narrow width of these peaks indicate a well-ordered and highly crystalline structure, reflecting the structural integrity of the compound. These results confirm that the synthesized $MnSO_4$ possesses a well-defined crystalline framework, demonstrating its stability and purity [9].

SEM of $MnSO_4$

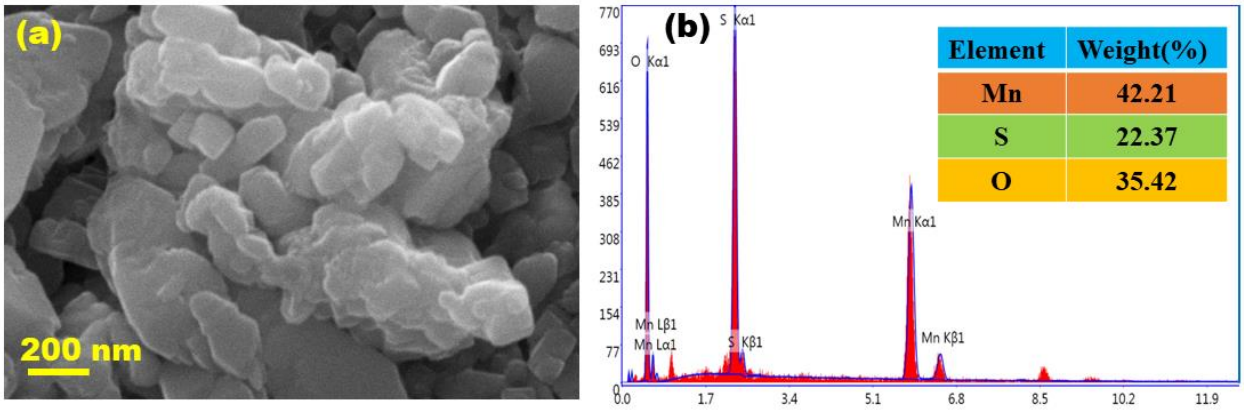

Fig. S3 (a) SEM and (b) EDX of $MnSO_4$

The SEM image (Fig S3) shows manganese sulfate ($MnSO_4$) exhibiting an agglomerated morphology with irregular and pellet-like shapes. The particles appear clustered and uneven in size, reflecting typical characteristics of nanoparticles formed through chemical synthesis routes.

This morphology suggests a high surface area due to the nanoscale particle size, which can enhance reactivity and surface-related properties [11,12]

The EDX pattern confirms the formation of $MnSO_4$ by showing the presence of the primary elements manganese (Mn), sulfur (S), and oxygen (O) with weight percentages of approximately 42.21%, 22.37%, and 35.42%, respectively, without any contamination. From the SEM EDX analysis it is clear that $MnSO_4$ successfully synthesized.

Reference

1 *Morphology and Chemical Purity of Water Suspension of Graphene Oxide FLAKES Aged for 14 Months in Ambient Conditions. A Preliminary Study - PMC, https://pmc.ncbi.nlm.nih.gov/articles/PMC8347880/, (accessed 1 September 2025).*

2 *N. M. S. Hidayah, W.-W. Liu, C.-W. Lai, N. Z. Noriman, C.-S. Khe, U. Hashim and H. C. Lee, Comparison on graphite, graphene oxide and reduced graphene oxide: Synthesis and characterization,* AIP Conf. Proc., *2017, **1892**, 150002.*

3 *F. T. Johra, J.-W. Lee and W.-G. Jung, Facile and safe graphene preparation on solution based platform,* J. Ind. Eng. Chem., *2014, **20**, 2883–2887.*

4 *H. Ahmad, M. T. Rahman, M. J. Faruki, S. R. Azzuhri, M. F. Ismail, N. M. S. Shah and M. Z. A. Razak, Graphene oxide (GO)-based wideband optical polarizer using a non-adiabatic microfiber,* J. Mod. Opt., *2017, **64**, 439–444.*

5 *I. Childres, L. A. Jauregui, W. Park, H. Cao and Y. P. Chen, RAMAN SPECTROSCOPY OF GRAPHENE AND RELATED MATERIALS.*

6 *P. Gangwar, S. Singh and N. Khare, Study of optical properties of graphene oxide and its derivatives using spectroscopic ellipsometry,* Appl. Phys. A, *2018, **124**, 620.*

7 *K.-Y. Shih, Y.-L. Kuan and E.-R. Wang, One-Step Microwave-Assisted Synthesis and Visible-Light Photocatalytic Activity Enhancement of BiOBr/RGO Nanocomposites for Degradation of Methylene Blue,* Materials, *2021, **14**, 4577.*

8 *N. Chadha, R. Sharma and P. Saini, A new insight into the structural modulation of graphene oxide upon chemical reduction probed by Raman spectroscopy and X-ray diffraction,* Carbon Lett., *2021, **31**, 1125–1131.*

9 *D. I. Jeong, S. Kim, J. S. Koo, S. Y. Lee, M. Kim, K. Y. Kim, M. O. K. Azad, M. Karmakar, S. Chu, B.-J. Chae, W.-S. Kang and H.-J. Cho, Manganese Sulfate Nanocomposites Fabricated by Hot-Melt Extrusion for Chemodynamic Therapy of Colorectal Cancer,* Pharmaceutics, *2023, **15**, 1831.*

10 P. Sagunthala, P. Yasotha and L. Vijaya, Growth and Characterization of Manganese (II) Sulphate and L-Lysine doped Manganese (II) Sulphate (LMnSO4) Crystals, Int. J. Sci. Eng. Appl.*, 2013, 46–52.*

11

12 G. Shahriar, G. G. R. Reza, L. Amir and Q. N. Ahmad, SYNTHESIS AND CHARACTERIZATION OF NANOPARTICLES MANGANESE (II) SULFATE MONOHYDRATE (MNSO4 .H2O).